ACTA NEUROBIOLOGIAE EXPERIMENTALIS

Research Paper Acta Neurobiol Exp 2008, 68: 10–25

Modulation of Ca^{2+} channel current by μ opioid receptors in prefrontal cortex pyramidal neurons in rats

Rafał Rola[1,2], Michał Jarkiewicz[1], and Paweł Szulczyk[1]*

[1]Department of Physiology and [2]Department of Experimental and Clinical Physiology, The Medical University of Warsaw, Krakowskie Przedmieście 26/28, 00-325 Warsaw, Poland, *Email: pawel.szulczyk@am.edu.pl

Our work assesses the effects of μ opioid receptor activation on high-threshold Ca^{2+}/Ba^{2+} currents in freshly dispersed pyramidal neurons of the medial prefrontal cortex in rats. Application of the specific μ receptor agonist (D-Ala^2, N-Me-Phe^4, Gly^5-ol)-enkephalin (DAMGO) at 1 μM decreased Ca^{2+} current amplitudes from 0.72 to 0.49 nA. The effect was abolished by naloxone and ω-Conotoxin GVIA. Inhibition was not abolished by strong depolarisation of the cell membrane. In addition, a macroscopic Ba^{2+} current recorded in cell-attached configuration was inhibited when DAMGO was applied outside the patch pipette. An adenylyl cyclase inhibitor (SQ 22536) and a protein kinase A inhibitor (H-89) decreased Ca^{2+} current amplitude. Moreover, the inhibitory effect of μ opioid receptors on Ca^{2+} currents required the activation of protein kinase A. We conclude that activation of μ opioid receptors in medial prefrontal cortex pyramidal neurons inhibits N type Ca^{2+} channel currents, and that protein kinase A is involved in this transduction pathway.

Key words: prefrontal cortex, pyramidal neurons, Ca^{2+} currents, Ba^{2+} currents, μ opioid receptors, PKA

INTRODUCTION

The prelimbic and infralimbic areas of the medial prefrontal cortex (mPFC), which receive dense dopaminergic input from the midbrain (Carr et al. 1999, Carr and Sesack 2000), are crucial for working memory in mammals (Williams and Castner 2006). It has been suggested that these areas are involved in higher cognitive processes, and that damage to them leads to devastating pathologies, including schizophrenia (Manoach 2003) and dementia (Rosen et al. 2005).

μ opioid receptors are widely distributed in the neocortex (Mansour et al. 1995), including the prefrontal cortex in humans (Schmidt et al. 2001, 2003). Recent neuroimaging studies in humans have indicated that μ opioid cortical transmission in the prefrontal cortex is tonically active (Zubieta et al. 2002), and participates in the organism's adaptation to pain and negative emotional states (Ribeiro et al. 2005). Moreover, cortical opioid transmission is involved in the regulation of mood. In particular, sadness states have been associated with a decrease in cortical cingulate μ opioid transmission (Zubieta et al. 2003).

Ca^{2+} ions are important second messengers which control numerous cellular effectors and influence the shape and activity pattern of action potentials (Carafoli 2002). One of the routes of Ca^{2+} entry into the intracellular compartment is *via* voltage-gated Ca^{2+} channels. Voltage-gated Ca^{2+} channels are negatively coupled to μ opioid receptors. For example, it was demonstrated that N-type (Rhim and Miller 1994, Wilding et al. 1995, Kim et al. 1997, Soldo and Moises 1997, Connor et al. 1999, Chieng and Bekkers 2001, Lee et al. 2004), and P- or Q-type Ca^{2+} currents (Rusin and Moises 1995) could be inhibited during activation of μ opioid receptors. Pyramidal neurons are the principal output cortical cells. Some pyramidal neurons of the prefrontal cortex express μ opioid receptors (Schmidt et al. 2001, 2003). Moreover, these neurons express N, L, P, Q and R high-threshold, voltage-dependent Ca^{2+} currents (Ishibashi et al. 1997, Day et al. 2002) and never or rarely display prominent low-threshold voltage-dependent Ca^{2+} currents (Lorenzon and Foehring 1995, Stewart et al. 1999, Day et al. 2002). Therefore, the

Correspondence should be addressed to P. Szulczyk, Email: pawel.szulczyk@am.edu.pl

Received 9 July 2007, accepted 10 December 2007

high-threshold Ca^{2+} channels in mPFC pyramidal cells are potential targets for μ opioid receptors.

Considering the importance of the mPFC for mammalian behavior and of μ opioid receptors for regulation of cell function, we decided to answer the following questions: Do μ opioid receptors modulate the voltage-dependent Ca^{2+} currents in infralimbic and prelimbic mPFC pyramidal neurons? If so, which subtype(s) of Ca^{2+} channels are controlled by μ opioid receptors? Which transduction pathway is involved in Ca^{2+} channel inhibition by μ opioid receptors?

METHODS

The animals and quantities used in this study conform to institutional and international guidelines on the ethical use of animals. Experiments were performed on young adult (2–3 week old) male Wistar rats (WAG Amk) obtained from a local animal house.

Cell dissections

Initially, the animals were decapitated. The brain was exposed, removed, and placed in an oxygenated, cold (4°C), artificial extracellular solution (mM): sucrose (234), KCl (2.5), NaH_2PO_4 (1), glucose (11), $MgSO_4$ (4), HEPES (N-(2-hydroxyethyl)piperazine-N'-(2-ethanesulfonic acid)) (15), $CaCl_2$ (0.1) pH 7.4 was adjusted with N-methyl-D-glucamine (NMDG), and osmolality was 330 mOsm/kg H_2O. Afterwards 400 μm coronal slices were prepared from the cerebral prefrontal tissue using a vibrotome (Vibrotome 1000, Pelco International, CA). Slices were placed in a solution containing (mM): NaCl (118), KCl (5.3), $CaCl_2$ (1.8), $MgSO_4$ (0.4), $NaHCO_3$ (26), NaH_2PO_4 (0.9), kynurenic acid (1), N-nitro-L-arginine (0.1), pyruvic acid (0.2), pH 7.4, and 310 mOsm/kg H_2O, bubbled with 95% O_2 and 5 % CO_2, at a temperature of 23–24°C, and stored until use (1–6 h).

Enzymatic and mechanical tissue dissociation

Parts of the slices 2.2–3.5 mm anterior to Bregma, 3–5 mm below the upper cortical surface and 0.1–0.9 mm from the midline (Kolb 1984, Berger et al. 1991), were dissected and transferred to a solution bubbled with O_2, containing (mM): NaCl (135), HEPES (10), KCl (5), $MgSO_4$ (1), glucose (10), pH 7.4 adjusted with NaOH, and 300 mOsm/kg H_2O with the addition of 1 mg/ml protease type XIV (Sigma). Enzymatic breakdown lasted 18 minutes at 32°C. In order to stop the enzyme action, the solution bathing the slices was replaced three times with an identically composed solution, but without the addition of enzymes. Parts of the slices corresponding to prelimbic and infralimbic areas (Öngür and Price 2000) were mechanically dispersed using Pasteur pipettes. The dispersed neurons were transferred to the recording chamber (type RC -24E, Warner Instruments LLC, USA) of a Nikon microscope (Nikon Instech Co., LTD, Kawasaki, Kanagawa, Japan). Cells were identified under Hoffman (magnification 400×). Recordings were acquired from distinctly three-dimensional, smooth surface pyramidal neurons with residual apical and basal dendrites and a short axon at the base (compare Fig. 1B in Witkowski and Szulczyk 2006).

Solutions

For voltage-clamp recordings in the whole cell configuration, the cells were initially perfused with an external solution containing (mM): NaCl (130), KCl (5), $MgCl_2$ (2), $CaCl_2$ (2), glucose (12) and HEPES (10). Its pH was adjusted to 7.4 with NaOH and the osmolality was 330 mOsm/kg H_2O. After the identification of a pyramidal neuron, the external solution was replaced with a solution designed to isolate the Ca^{2+} currents. It contained (mM): methanesulfonic acid (145), TEA-OH (tetraethylammonium hydroxide, 145), HEPES (10), $CaCl_2$ (10) (or $BaCl_2$, 5 mM), glucose (15) and TTX (Tetrodotoxin, 0.002). The pH was adjusted to 7.4 with TEA-OH and the osmolality was 330 mOsm/kg H_2O. The internal solution contained (mM): NMDG (90), TEA-Cl (tetraethylammonium chloride, 20), HEPES-Cl (40), sucrose (20), MgATP (adenosino 5'-triphosphate magnesium salt, 2), Na_2GTP (guanosine 5'-triphosphate disodium salt, 0.3), phosphocreatine (14), EGTA (ethylene glycol- bis-(2-aminoethylether)-N,N,N',N'-tetraacetic acid, 11), and $CaCl_2$ (1) which maintained internal Ca^{2+} at 10 nM. The pH was adjusted with HCl to 7.4 and the osmolality with sucrose to 276 mOsm/kg H_2O.

For voltage-clamp recordings in the cell-attached configuration, the external solution (outside of the pipette) consisted of (mM): K aspartate (140), HEPES (10), glucose (10), $MgCl_2 \times 6H_20$ (2), EGTA

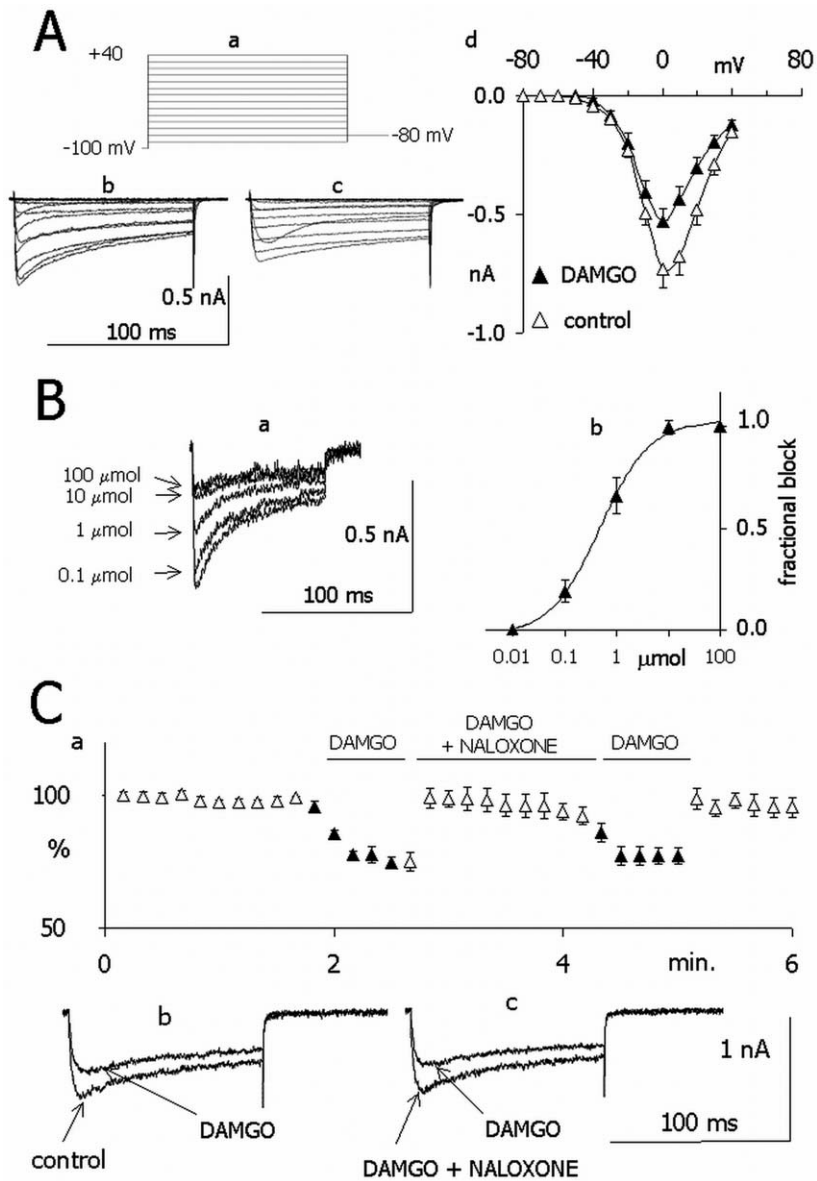

Fig. 1. Effect of DAMGO on Ca^{2+} currents. (A) (a) Voltage protocol applied to study I/V relationships. Currents were evoked by voltage steps from –90 to +40 mV in 10 mV increments, lasting 100 ms. Each step was preceded by a hyperpolarization to –100 mV, lasting 1 s. The holding potential was –80 mV. Original traces evoked by this voltage protocol were recorded before (b) and during (c) DAMGO application. (d) I/V relationships showing average peak Ca^{2+} currents evoked by the voltage steps shown in (Aa). Peak current amplitudes (ordinate) were plotted against the amplitude of the voltage step (abscissa). (B) (a) Original overlapping Ca^{2+} current traces obtained from 1 neuron before and after the application of different concentrations of DAMGO. The current traces were labelled with the corresponding concentrations of applied DAMGO. (b) Dose-response curve of Ca^{2+} current inhibition by DAMGO. On the vertical axis is the normalized difference between control current amplitude and current amplitude measured during application of DAMGO (at different concentrations). Abscissa – DAMGO concentrations. (C) (a) Normalized Ca^{2+} current amplitudes recorded before and during application of DAMGO, DAMGO and naloxone, and DAMGO alone . Ordinate – normalized current amplitude; abscissa – time in minutes. (b) Original current traces recorded before (control) and during DAMGO application (DAMGO). (c) Current traces recorded during application of DAMGO and naloxone (DAMGO + naloxone) and during repeated DAMGO applications (DAMGO). Currents were evoked once every 10 seconds by a 100 ms voltage step to 0 mV, preceded by a –100 mV prepulse lasting 1 s. The holding potential was –80 mV. In this and other figures, open markers indicate measurements obtained before DAMGO application, while filled markers indicate measurements during application. Horizontal lines mark applications.

(2), TTX (0.003). The pH (7.4) was adjusted with NMDG and the osmolality (320 mOsm/kg H_2O) with sucrose. In this external solution, the membrane potential of the tested cells was clamped at approximately 0 mV (compare Verheugen et al. 1999). The solution in the pipette contained: Ba acetate (100), $BaCl_2$ (10), CsCl (5), HEPES (10), TEA-Cl (5), TTX (0.003), nifedipine (10 μM) and ω-Agatoxin IVA (0.2 μM). The pH (7.4) was adjusted with TEA-OH and osmolality (340 mOsm/kg H_2O) was adjusted with sucrose.

Drug delivery

DAMGO ([D-Ala^2, N-Me-Phe^4, Gly^5-ol]-enkephalin), naloxone, chelerythrine chloride, H-89 (N-[2-(p-Bromocinnamylamino)ethyl]-5-isoquinolinesulfonamide dihydrochloride) and SQ 22536 (9-(Tetrahydro-2-furanyl)-9H-purin-6-amine; 9-THF-Ade) were dissolved in distilled water and stored at –20°C. PMA (phorbol 12-myristate-13-acetate) and forskolin was dissolved in DMSO and stored at –20°C. PMA and chelerythrine chloride were stored and applied in the dark. Forskolin, DAMGO, naloxone, chelerythrine chloride, H-89 and SQ 22536 were applied extracellularly. GDP-β-S (guanosine 5'-β-thiodiphosphate) was dissolved in distilled water and stored as 10 μl stock solutions at –70°C for 3 weeks. In some experiments, 0.4 mM GDP-β-S was replaced for 0.4 mM Na_2GTP in intracellular solution.

Chemical compounds dissolved in the extracellular solution were delivered to the cell *via* a gravity-fed large bore pipette (EVH-9, Bio-Logic Science Instruments, France).

Toxins were diluted directly in the bath solution, while nifedipine was first dissolved in 0.2% ethanol and 0.1% polyethylene glycol. 10 μM of nifedipine, 5 μM of ω-Conotoxin GVIA, 0.2 μM of ω-Agatoxin IVA, and 5 μM of $LaCl_3$ or 200 μM of $CdCl_2$ were used for blocking Ca^{2+} currents. The blockers were applied in random order with the exception of $LaCl_3$, which was applied last. The majority of the chemical compounds were purchased from SIGMA-ALDRICH. Chelerythrine chloride, forskolin and naloxone were purchased from TOCRIS COOKSON (GB). Toxins were purchased from Peptide Institute, Inc. (Japan) and TTX was from Alomone Labs (Israel).

Current recordings

The experiments were performed at room temperature (21–23°C). The voltage-clamp recordings were carried out in the whole-cell and cell attached configuration using an Axopatch 1D amplifier (Axon Inst., Foster City, CA). pClamp software was used. The pipettes were fabricated from borosilicate glass capillaries (O.D. 1.2 mm, I.D. 0.9 mm – Hilgenberg or O.D. 1.2 mm, I.D. 0.69 mm – Harward Apparatus Ltd.) using a P-87 puller (Sutter Instruments, Inc., CA) and were fire-polished. The junction potential was nulled with the pipette tip immersed in the bath.

In order to perform recordings in whole-cell configuration, patch pipettes were sealed against the cell membrane and the membrane was subsequently disrupted by suction. The electrode capacitance was compensated by the circuit of the amplifier. A holding potential of –80 mV was applied. Cell capacitance and series resistance were estimated from the decay of the capacitance transient induced by a ±10 mV pulse from the holding potential. A series resistance compensation of 80% was applied. A P/4 protocol was used. The open tip resistance of pipettes filled with intracellular fluid and placed in the extracellular solution was 2.2 ± 0.07 MΩ, access resistance was 6.31 ± 0.2 MΩ, the recorded maximum current amounted to 0.72 ± 0.04 nA, and the calculated maximum voltage clamp error after series resistance compensation (80%) was 1.2 ± 0.04 mV (n=153). The maximum encountered voltage clamp error in a single cell was 5.4 mV. A similar method of Ca^{2+} current recording was applied in our earlier studies (Kukwa et al. 1998, 2000, Rola et al. 2003).

The pipettes used in the cell-attached configuration were also covered with Sylgard (Dow Corning Corporation Midland, MI). In these recordings the overall frequency response was set at 2 kHz and analog signal was digitized at 10 kHz. When recordings were performed in the cell-attached configuration, steady-state passive current was removed from the data off-line using the leak subtraction utility of the pClamp software.

Data analysis

During drug delivery, the Ca^{2+} currents recorded in the whole cell configuration were analyzed as follows. Before, during, and after a tested compound

delivery, the Ca^{2+} currents were evoked once every 10 seconds by a voltage step to 0 mV lasting 100 ms, preceded by a –100 mV prepulse lasting 1 s. The holding potential was –80 mV. The maximum current amplitudes were measured, normalized and plotted as a function of time. In order to compare a response to the applied compound with control data, the last five measurements obtained during drug application were averaged and expressed as a percentage of the average of the last five measurements obtained in control conditions (Figs 1Ca, 2C, 3B, 4B, 5A).

A sigmoidal dose-response function in the form $I_1+(I_2-I_1)/(1+10\text{^}((\log X_1-X)p)$ was used to determine the half blocking DAMGO concentration, where I_1 and I_2 are initial and final amplitudes, X_1 is the half blocking concentration, X is the logarithm of DAMGO concentration, and p is the Hill coefficient.

All results presented throughout the paper and in the Figures are shown as Means ± SEM. Even though data sets did not appear to deviate from a normal distribution, we decided to apply nonparametric tests because, in the majority of cases, a small number of neurons were tested. For repeated measures analysis, the Friedman test (nonparametric repeated measures ANOVA) was performed followed by the *post-hoc* Dunn test. The Wilcoxon test for matched pairs was used when comparing two groups. In one case, the Student's *t*-Test was applied (marked in the text).

RESULTS

Ca^{2+} currents were recorded in 141 mPFC pyramidal neurons in the whole cell configuration. Four cells expressed low-threshold (~ –60 mV), fast inactivating, presumably T-type currents in addition to high-threshold Ca^{2+} currents. In these cells, the properties of Ca^{2+} currents were not further analysed.

Do μ opioid receptors modulate voltage-dependent Ca^{2+} currents in mPFC pyramidal neurons?

The effect of DAMGO on voltage-gated Ca^{2+} currents was tested. Original recordings of Ca^{2+} currents evoked by the voltage protocol shown in Fig. 1Aa before and during application of 1 μM DAMGO are demonstrated in Fig. 1Ab–Ac. The I/V relationships indicate that the peak current amplitude significantly decreased after DAMGO application (from 100% to 72.25% ± 3.5%, $P<0.01$, $n=14$, Fig. 1Ad). Application of different DAMGO concentrations, from 0.01 μM to 100 μM, decreased the Ca^{2+} current amplitude in a concentration-dependent manner (Fig. 1Ba). The EC_{50} was 0.48 ± 0.06 μM ($n=10$; Fig. 1Bb). In the tests described below, 1 μM DAMGO was applied.

DAMGO-induced inhibition was abolished by naloxone. For example, application of DAMGO decreased the peak current amplitude from 100% to 74.2 ± 2.8% ($P<0.01$, $Fr=16.22$, $n=9$, Fig. 1Ca,b). When naloxone (10 mM) was applied along with DAMGO, the Ca^{2+} current amplitude recovered to 97.2 ± 3.0% ($P>0.05$, $Fr=16.22$, $n=9$, Fig. 1Ca). With the removal of naloxone in the continuous presence of DAMGO, the current amplitude decreased again to 77.2 ± 3.0% ($P<0.05$, $n=5$, Fig. 1Ca,c).

In all pyramidal neurons tested, DAMGO decreased the peak Ca^{2+} current amplitude (from 0.72 ± 0.03 nA (100%) to 0.49 ± 0.02 nA (68.06%), $P<0.001$, Student's *t*-Test, $n=137$).

Which subtype(s) of Ca^{2+} channels are controlled by μ opioid receptors?

Application of ω-Conotoxin GVIA (5 μM), ω-Agatoxin IVA (0.2 μM), nifedipine (10 μM) and $LaCl_3$ (5 μM) blocked, respectively, 25.2 ± 0.7%, 20.5 ± 3.0%, 14.2 ± 1.5% and 29.4 ± 2.2% ($n=8$) of the Ca^{2+} current in mPFC neurons. An example of current amplitude decrease and original recordings (inset) are shown in Fig. 2A.

In 7 neurons, concurrent application of ω-Agatoxin IVA and nifedipine significantly decreased the Ca^{2+} current amplitude from control (100%) to 59.6 ± 5.9% ($P<0.01$, ω-Agatoxin IVA + nifedipine). Additional application of DAMGO further decreased the current amplitude to 37.5 ± 3.9% ($P<0.01$, ω-Agatoxin IVA + nifedipine + DAMGO). Hence, Ca^{2+} current inhibition by ω-Agatoxin IVA and nifedipine did not eliminate inhibition of the Ca^{2+} current by DAMGO (Fig. 2Ba).

In 6 neurons, ω-Conotoxin GVIA (5 μM) was applied first and decreased the Ca^{2+} current amplitude from control (100%) to 76.0 ± 9.0% (ω-Conotoxin GVIA). Additional application of DAMGO did not significantly change the current amplitude as compared to the level recorded during toxin-only application (71.0 ± 11% of the control, $P>0.05$, ω-Conotoxin

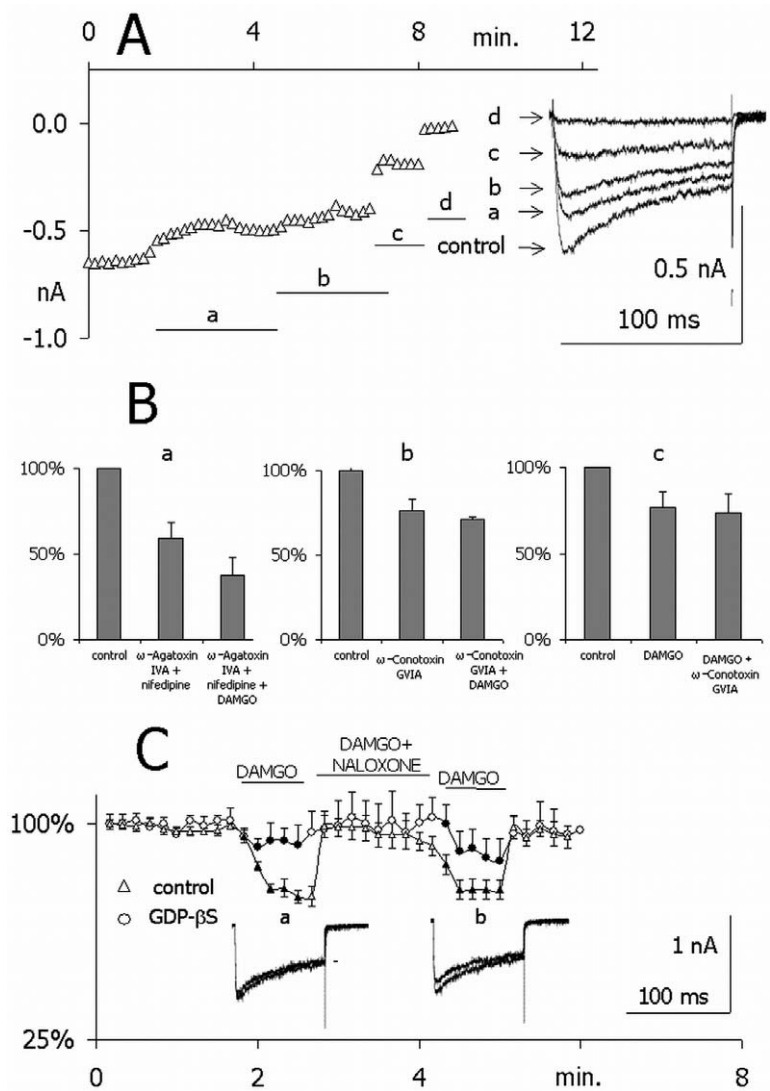

Fig. 2. Components of the voltage-activated Ca^{2+} current. The effect of GDP-β-S on Ca^{2+} current. (A) Inhibition of Ca^{2+} currents evoked in a single neuron by ω-Conotoxin GVIA [(a) 5 μM], nifedipine [(b) 10 μM], ω-Agatoxin IVA [(c) 0.2 μM] and $LaCl_3$ [(d) 5μM]. The maximum current amplitudes and responses to the application of Ca^{2+} channel inhibitors are plotted on the ordinate against time (abscissa). Original recordings of Ca^{2+} currents during the application of Ca^{2+} channel inhibitors are shown in the inset. (B) (a) Relative amplitudes of Ca^{2+} current recordings before application of inhibitors (control), during application of ω-Agatoxin IVA and nifedipine (ω-Agatoxin IVA + nifedipine) and during application of ω-Agatoxin IVA, nifedipine and DAMGO (ω-Agatoxin IVA + nifedipine + DAMGO). (b) Relative amplitudes of Ca^{2+} current recordings before application of inhibitors (control), during application of ω-Conotoxin GVIA (ω-Conotoxin GVIA) and during application of ω-Conotoxin GVIA and DAMGO (ω-Conotoxin GVIA + DAMGO). (c) Relative amplitudes of Ca^{2+} current recordings before inhibitor application (control), during DAMGO application (DAMGO) and during application of DAMGO and ω-Conotoxin GVIA (DAMGO + ω-Conotoxin GVIA). (C) Effect of intracellular GDP-β-S on DAMGO-induced Ca^{2+} current inhibition. Normalized Ca^{2+} current amplitude was plotted on the vertical axis. Applications of DAMGO or both DAMGO and naloxone together are marked in the figure. Recordings with and without GDP-β-S in the intracellular solution are marked with points and triangles, respectively. Current recordings obtained in the absence of GDP-β-S and the presence of GTP in the intracellular solution were taken from Figure 1C. Insets: original recordings obtained before and during DAMGO application with GDP-β-S in the intracellular solution: (a) shows the first DAMGO application, and (b) shows the second one. Ca^{2+} currents were evoked once every 10 seconds by a voltage step to 0 mV lasting 100 ms, preceded by a –100 mV prepulse lasting 1 s. The holding potential was –80 mV.

GVIA + DAMGO). Therefore, the inhibitory effect of DAMGO was not observed after prior application of ω-Conotoxin GVIA (Fig. 2Bb).

In another group of 5 neurons, DAMGO decreased the Ca^{2+} current amplitude from control (100%) to 77.0 ± 6.0% (DAMGO). Additional application of ω-Conotoxin GVIA (5 μM) did not decrease the current amplitude any further (74.0 ± 8.0%, $P>0.05$, DAMGO + ω-Conotoxin GVIA). Therefore, when the Ca^{2+} current component sensitive to DAMGO was eliminated, the inhibitory effect of ω-Conotoxin G-VIA was abolished (Fig. 2Bc).

What is the mechanism of signal transduction from μ opioid receptors to Ca^{2+} channels?

In the presence of GDP-β-S and the absence of GTP in the pipette (intracellular) solution, the Ca^{2+} current amplitude did not change significantly with DAMGO application, decreasing slightly from 100% to 94.5 ± 3.0% [Fig. 2C, points, inset (a), n=6, DAMGO, Fr=0.2, $P>0.05$]. When DAMGO was applied along with naloxone (10 μM), the current amplitude reached a level of 96.7 ± 4.3% of the control (Fig. 2C, points DAMGO + naloxone, n=6, Fr=0.2, $P>0.05$). When naloxone was removed and DAMGO alone was applied, the current amplitude did not change significantly [Fig. 2C, points, inset (b), 90.2 ± 4.2%, n=6, Fr=0.2, $P>0.05$]. Figure 2C also demonstrates the inhibitory effects of DAMGO on Ca^{2+} currents in the presence of GTP and absence of GDP-β-S in the intracellular solution (results taken from Fig. 1C – triangles). These data indicate that a G protein-coupled pathway is involved in Ca^{2+} current inhibition in mPFC pyramidal neurons.

In order to test whether the DAMGO-induced inhibition of Ca^{2+} currents was sensitive to large-amplitude depolarisation, we applied test pulses to 0 mV lasting 20 ms before and after a large depolarising pulse to +80 mV lasting 50 ms (Fig. 3Aa). This stimulus protocol was applied once every 10 seconds. Without DAMGO application, the amplitudes of the Ca^{2+} currents evoked by test pulses before a large depolarisation (100%) and afterwards (86.6 ± 16.0%, $P>0.05$) were not significantly different (Fig.3Ab, Control, n=16, $P>0.05$). Similar results were obtained during DAMGO application (Fig. 3Ab, DAMGO, 100% vs. 95.1 ± 2.8%, n=16, $P>0.05$). During DAMGO application, the Ca^{2+} current evoked by the second test step was still inhibited to 66 ± 8.3% of control levels (n=16, $P<0.05$) (Fig. 3Ab, 3B Ca^{2+}).

The stimulus protocol shown in Fig. 3Aa was repeated with Ba^{2+} ions replacing Ca^{2+} as a charge carrier in the extracellular solution. In these experiments, the amplitude of the large depolarisation was diminished (+60 mV instead of +80 mV), and the concentration of charge carrier was lowered to 5 mM in order to achieve better control of the deactivating Ba^{2+} current evoked by a voltage step.

In the absence of DAMGO, the Ba^{2+} current amplitude recorded after the large voltage step was significantly larger compared to the amplitude recorded before (100% before vs. 122.1 ± 10.5% after, $P<0.05$, n=11, Fig. 3Ac, control). Also during DAMGO application, current amplitude increased after a large voltage step (100% vs. 123.4 ± 12.5% $P<0.05$, n=11, Fig. 3Ac, DAMGO). These results indicate that the Ba^{2+} current was less subject to inhibition after a large voltage step, irrespective of whether DAMGO was applied or not.

Inspection of Fig. 3Ac indicates that the Ba^{2+} current inactivated in a time-dependent manner markedly faster after, rather than before, a large voltage step. This effect was observed in 8 of 11 Ba^{2+} current recordings and was never seen when Ca^{2+} currents were recorded (n=16). The time constant of Ba^{2+} current inactivation decreased from 24.4 ± 1.3 ms to 13.3 ± 1.9 ms ($P<0.01$, n=8) without DAMGO application, and from 29.5 ± 2.4 ms to 14.5 ± 0.4 ms ($P<0.01$, n=8) when DAMGO was applied.

Figure 3B (Ba^{2+}) shows Ba^{2+} currents evoked by the pulse, which followed a large cell membrane depolarisation before and during DAMGO application and during washout. DAMGO inhibited Ba^{2+} currents to 57.9 ± 8.4% (n=11, $P<0.01$) of control levels.

We also recorded macroscopic Ba^{2+} currents in the cell-attached configuration before and after application of DAMGO to the cell outside of the pipette. Ba^{2+} ions (110 mM) were applied to the pipette as charge carrier (Fig. 3C). Ramp depolarisation of the patched membrane from –60 mV to +60 mV over 500 ms (Fig. 3Ca), applied once every 2 s, evoked inward currents (Fig. 3Cb control). We first wanted to confirm that Ba^{2+} currents flowing through Ca^{2+} channels were recorded under these conditions. The solution in the shank contained an inorganic Ca^{2+} channel blocker (Cd^{2+}, 0.2 mM), while the recording pipette tip contained a solution without Cd^{2+}. Inward Ba^{2+} currents flowing

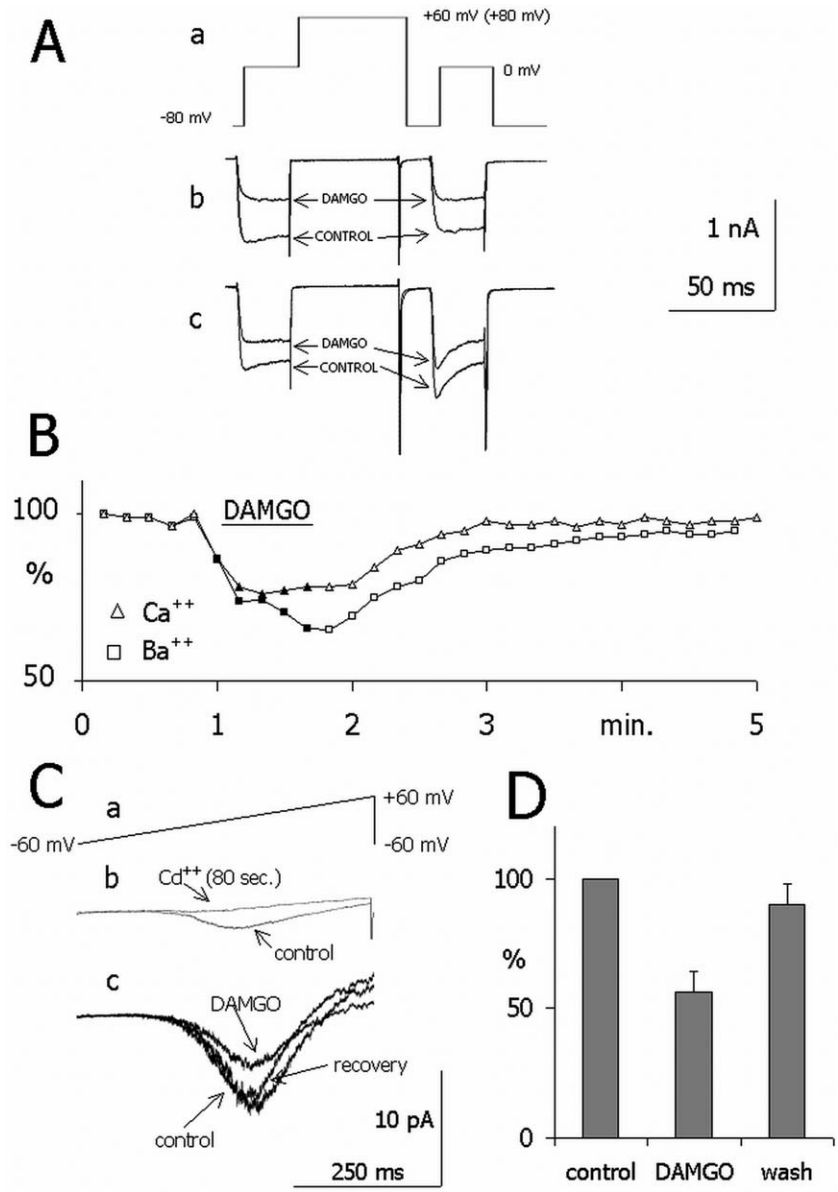

Fig. 3. Effects of large amplitude depolarisations on Ca^{2+} and Ba^{2+} currents and effect of DAMGO on Ba^{2+} currents recorded in cell-attached configuration. (A) (a) Voltage protocol applied to study the effects of large membrane depolarisations on Ca^{2+} and Ba^{2+} currents. The protocol was applied once every 10 seconds and consisted of two identical test pulses lasting 25 ms (to 0 mV from a holding potential of –80 mV) separated by a pulse to +80 mV (for Ca^{2+} currents) or to +60 mV (for Ba^{2+} currents), lasting 50 ms. In order to avoid a marked stimulus artifact, the membrane potential was stepped back to –80 mV for 15 ms before a second test pulse. (b) Original recordings of Ca^{2+} currents in response to the protocol shown in (Aa) before DAMGO application (control) and during DAMGO application (DAMGO). (c) Original recordings of Ba^{2+} currents in response to the protocol shown in (Aa) before DAMGO application (control) and during DAMGO application (DAMGO). (B) The amplitudes of the Ca^{2+} (triangles) and Ba^{2+} currents (squares) evoked by pulses applied after large membrane depolarisations [compare (Ab) and (Ac)]. Measurements were obtained before, during and after DAMGO washout. Ordinate – amplitude of the recorded current. Abscissa – time in minutes. (C) (a) A voltage ramp from –60 mV to +60 mV lasting 500 ms (holding –60 mV), which was applied to the patch in order to record Ba^{2+} currents. (b) Currents were recorded before (control) and after complete suppression of current by Cd^{2+} (80 s). Ten current sweeps were averaged. (c) Currents recorded before (control) and after DAMGO application (DAMGO) and DAMGO washout (recovery). Each trace represents 5 averaged sweeps. In (b) and (c), currents were evoked by the voltage protocol shown in (a). (D) Relative maximum amplitude of Ba^{2+} currents recorded in cell-attached configuration under control conditions (control), during DAMGO application (DAMGO) and after washout (wash).

through the patch (Fig. 3Cb control) were abolished 80 s after pipette sealing (Fig. 3Cb, Cd^{2+} 80 s). Cd^{2+} probably diffused to the pipette tip and blocked Ca^{2+} channels (Ba^{2+} patch current). In this experimental configuration, the effect of DAMGO on the Ba^{2+} patch current was tested. During this test, the pipette solution contained blockers specific to P- and Q-type Ca^{2+} channels (ω-Agatoxin IVA, 0.2 μM) and L-type channels (nifedipine, 10 μM). In 7 cells, application of DAMGO to the cell membrane outside the patch significantly decreased the Ba^{2+} patch current from 100% (control) to 56.1 ± 2.7% (DAMGO, Fr=17.54, P<0.001). The current recovered after washout to 90.1 ± 2.5% of the control (Fig. 3Cc, recovery, Fr=17.54, P>0.05 with respect to the control).

Effect of PKA and PKC on Ca^{2+} current inhibition by DAMGO

In order to test whether PKA was involved in Ca^{2+} current inhibition by DAMGO in mPFC pyramidal neurons, Ca^{2+} currents were recorded in conventional whole cell configuration. The effect of the adenylyl cyclase activator forskolin (10 μM) on DAMGO-inhibited Ca^{2+} currents was tested in 3 experiments. Before forskolin application, DAMGO decreased Ca^{2+} current amplitudes to 75.0%, 85.2% and 70.6% of control, while during the addition of forskolin, DAMGO reduced calcium current amplitudes to 71.2%, 86.6% and 66.9%, respectively (Fig. 4A). Original recordings of Ca^{2+} currents during application of (a) DAMGO and (b) DAMGO with forskolin versus control are shown in Figure 4A. Application of forskolin alone did not affect Ca^{2+} current amplitude.

Application of adenylyl cyclase inhibitor, SQ 22536 (100 μM), decreased Ca^{2+} current amplitude significantly from 100% (control) to 63.2 ± 7.0% (n=6, Fr=9.0, P<0.05). During Ca^{2+} current inhibition by SQ 22536, additional application of DAMGO did not change Ca^{2+} current amplitude (62.2 ± 6.2%). DAMGO applied alone (without SQ 22536) decreased Ca^{2+} currents to 79.3 ± 5.1% (Fig. 4B, Fr=9.0, P<0.05). Insets to Figure 4B show current traces recorded before and during DAMGO application without (a) and with (b) SQ 22536.

Next, H-89 was applied in order to inhibit PKA directly. Each application of H-89 or H-89 together with 1 μM DAMGO was preceded by a reference application of DAMGO (1 μM) alone. H-89 was applied at the following concentrations: 0.01 μM (points, n=7), 0.1 μM (squares, n=5) and 1.0 μM (triangles, n=6, Fig. 5A). Original Ca^{2+} current recordings before and after application of (a) DAMGO, (b) H-89 (0.1 μM), or (c) both DAMGO and H-89 (0.1 μM) are shown in Fig. 5Ba,b,c. Original Ca^{2+} current recordings before and after application of (d) DAMGO, (e) H-89 (1.0 μM), and (f) both DAMGO and H-89 (1.0 μM) are shown in Fig. 5Bd,e,f. Application of either DAMGO alone or DAMGO together with different concentrations of H-89 decreased the Ca^{2+} current amplitude to the same levels, 76.2 ± 3.1% and 72.1 ± 2.6%, respectively, relative to the current amplitude before the first DAMGO application (0.01 μM H-89; Fr=10.8, P>0.05); 67.4 ± 3.2% and 63.2 ± 4.3% (0.1 μM H-89; Fr=8.5, P>0.05); and 72.2 ± 2.0% and 60.3 ± 5.1% (1.0 μM H-89; Fr=10.2, P>0.05) (Fig. 5A).

We were interested which fraction of the amplitude decrease evoked by the application of DAMGO alone was suppressed by H-89 applied alone, and which by application of DAMGO in addition to H-89. It was found that H-89 applied at a concentration of 0.01 μM suppressed 22.6 ± 4.5% of the total Ca^{2+} current inhibited by the preliminary DAMGO application. Addition of DAMGO inhibited the remaining 77.4 ± 6.5% of the total current inhibited by the first DAMGO application (n=7, Fig. 5Ca). H-89 at a concentration of 0.1 μM inhibited 67.6 ± 4.2% of the total Ca^{2+} current suppressed by the first DAMGO application. Additional application of DAMGO inhibited 32.4 ± 4.0% of the total current suppressed by the first DAMGO application (n=5, Fig.5Cc, Bc). Finally, H-89 at a concentration of 1 μM inhibited 98.0 ± 4.2% of the total current suppressed by the first DAMGO application. Additional DAMGO application did not inhibit the Ca^{2+} current any further (suppression of 2 ± 3.8% of the total current inhibited by first DAMGO application, n=6, Fig. 5Cd, 5Bf).

We also tested the effects of a PKC activator and inhibitor on Ca^{2+} current inhibition by DAMGO (not shown). A 4-minute application of 3 μM chelerythrine chloride, a PKC inhibitor, did not significantly change the current inhibition by DAMGO. Before and during chelerythrine chloride application, DAMGO decreased the current amplitude, respectively, to 77.3 ± 2.0% and 79.5 ± 3.0% of the pre-application level (n=6, Fr=9.33, P>0.05). The same experiment was repeated with chelerythrine chloride at 9 μM.

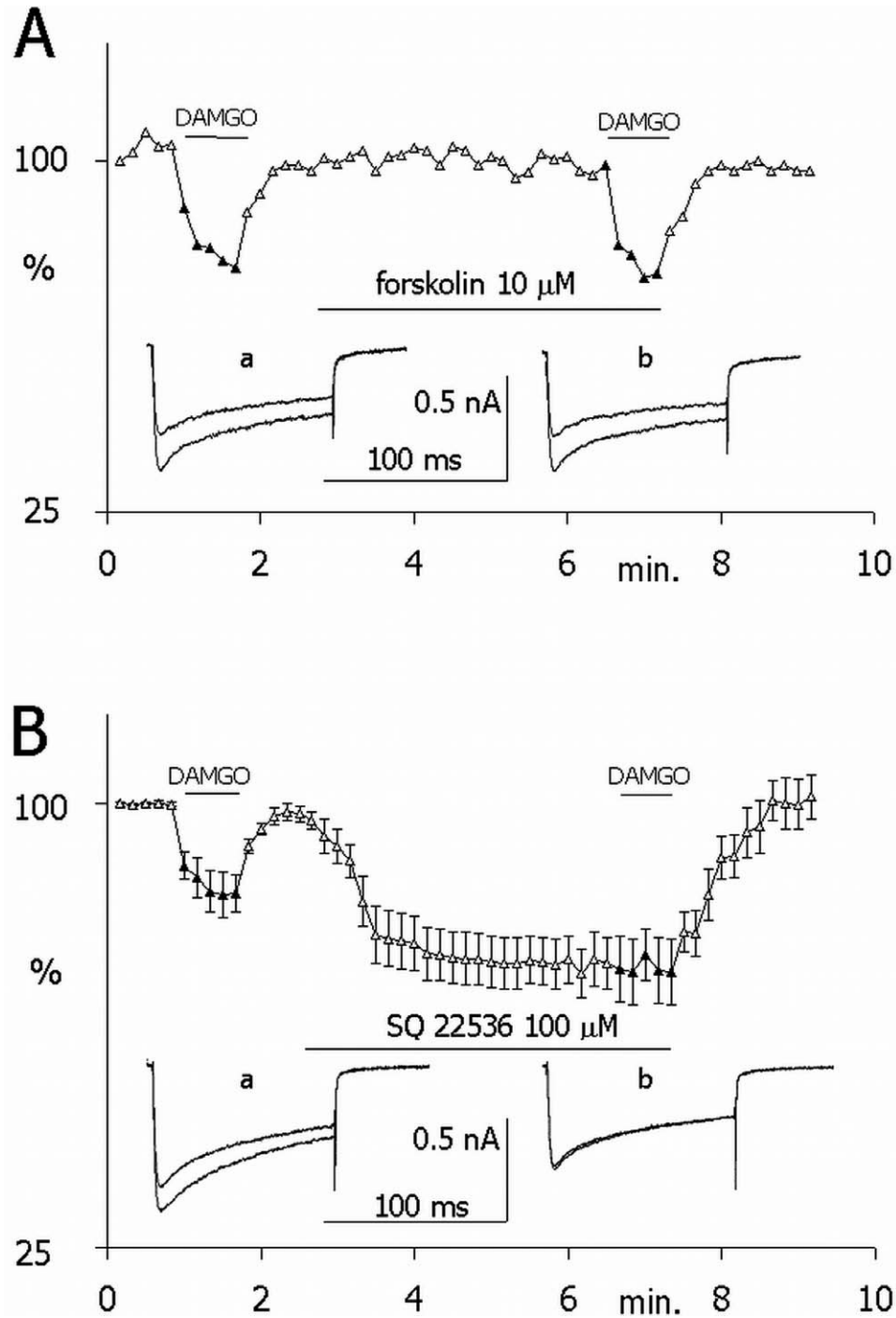

Fig. 4. Effects of an adenylyl cyclase activator and inhibitor on the Ca^{2+} current. (A) Effects of DAMGO and DAMGO applied together with the adenylyl cyclase activator forskolin (10 μM) on the normalized amplitudes of Ca^{2+} currents (ordinate). Abscissa – time in minutes. Insets – overlapping Ca^{2+} current traces recorded (a) before and during the first DAMGO application, and (b) before and during DAMGO application while the cell was superfused with forskolin. (B) Effects of DAMGO and DAMGO applied together with the adenylyl cyclase inhibitor SQ 22536 (100 μM) on the normalized amplitudes of Ca^{2+} currents (ordinate). Abscissa – time in minutes. Insets – overlapping Ca^{2+} current traces recorded (a) before and during the first DAMGO application, and (b) before and during DAMGO application while the cell was superfused with SQ 22536. In (A) and (B), currents were evoked by a voltage step to 0 mV lasting 100 ms, preceded by a –100 mV prepulse lasting 1 s. The currents were evoked once every 10 seconds.

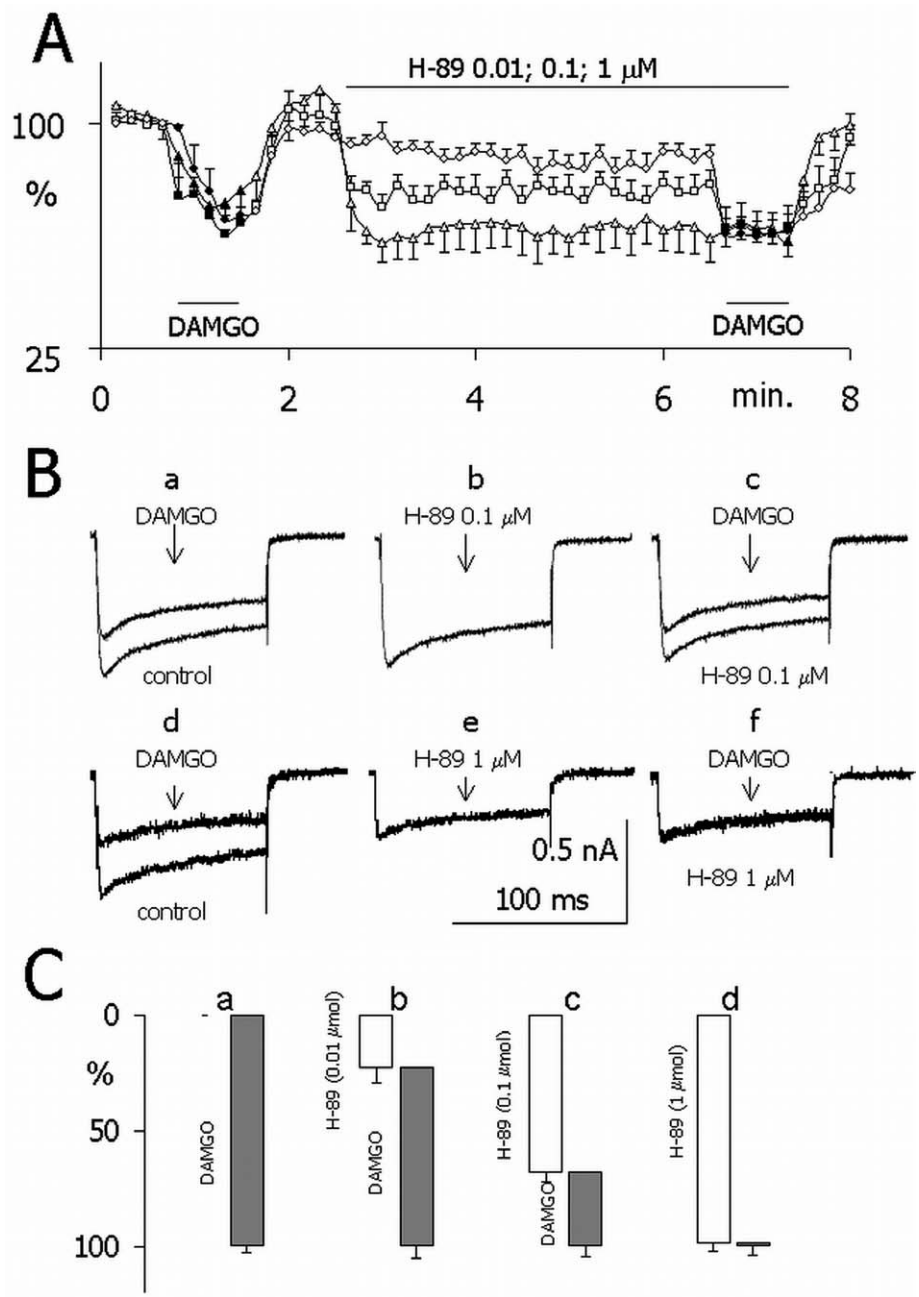

Fig. 5. Control of Ca^{2+} currents by a PKA inhibitor. (A) Effect of DAMGO (DAMGO) and H-89 on the normalized amplitudes of Ca^{2+} currents (ordinate). The results with different concentrations of H-89 are shown as points (0.01 μM), squares (0.1 μM) and triangles (1 μM). Abscissa – time in minutes. DAMGO was applied twice, before and during H-89 application in concentrations of 0.01 μM, 0.1 μM, and 1 μM. (B) Original, overlapping Ca^{2+} current traces recorded before and during DAMGO application (a,d), during the application of H-89 in concentrations of 0.1 and 1.0 μM [(b), (e)] and before and during the application of DAMGO while the cell was superfused with H-89 [0.1 μM, 1 μM; (c), (f)]. (C) Fraction of the current inhibited by H-89 and DAMGO. (a) It was assumed that the amplitude of the current inhibited by the first DAMGO application in (A) was 100%. (b) Fraction of the current inhibited by H-89 alone (0.01 μM) and DAMGO (1 μM) superimposed on H-89 (0.01 μM). (c) Fraction of the current inhibited by H-89 alone (0.1 μM) and DAMGO (1 μM) superimposed on H-89 (0.1 μM). (d) Fraction of the current inhibited by H-89 alone (1 μM) and DAMGO (1 μM) superimposed on H-89 (1 μM). Currents were evoked by a voltage step to 0 mV lasting 100 ms, preceded by a –100 mV prepulse lasting 1 s. Currents were evoked once every 10 seconds and continuously recorded. The holding potential was –80 mV.

DAMGO inhibited Ca^{2+} current to the same level before (72.0 ± 3.0%) and during (71 ± 4.0%) chelerythrine chloride application (Fr=8.28, P>0.05, n=5). When chelerythrine chloride was applied alone at concentrations of 3 μM or 9 μM between DAMGO applications, the Ca^{2+} current amplitude remained unaffected.

The effect of the PKC activator PMA (1 μM, 4 minutes) on Ca^{2+} currents was tested in 3 experiments. DAMGO applied alone decreased current amplitude to 84.0%, 68.5% and 73.0% of the pre-application level. During PMA application, DAMGO decreased the current amplitude, respectively, to 81.2%, 79.5% and 82.3% of the pre-application level. Therefore, application of PMA did not markedly affect inhibition of Ca^{2+} currents by DAMGO.

DISCUSSION

This study demonstrates that activation of μ opioid receptors reproducibly decreases voltage-dependent Ca^{2+} currents in pyramidal neurons in the prelimbic and infralimbic areas of the mPFC. The signal transduction involves the cAMP/PKA signalling pathway.

Type of Ca^{2+} channel inhibited by μ opioid receptors

As reported in other studies (Lorenzon and Foehring 1995, Ishibashi et al. 1997, Stewart et al. 1999, Day et al. 2002), we found that mPFC pyramidal neurons express the L, N, P/Q and R subtypes of Ca^{2+} channels. Inhibition of Ca^{2+} current by DAMGO was abolished by prior application of an N channel blocker, and a preceding DAMGO application abolished the effect of this blocker. In contrast, the inhibitory effect of DAMGO was still observed after prior application of L and P/Q channel blockers. Hence, in the pyramidal neurons of the mPFC, DAMGO application inhibited N-type Ca^{2+} currents.

What is the mechanism of signal transduction?

In order to test whether G-proteins are involved in the transduction pathway, GDP-β-S, a non-hydrolysable GDP analog, was applied to the cell. It is assumed that GDP-β-S irreversibly binds to G-proteins, thereby blocking receptor-mediated activation (Holz et al. 1986). The opioid-dependent inhibition of Ca^{2+} channels was abolished in the presence of GDP-β-S, which suggests that the Ca^{2+} current inhibition is G-protein-dependent.

We expected that activation of μ opioid receptors would lead to inhibition of Ca^{2+} channel currents by the release of the βγ subunit from the activated Gi/o protein and the direct interaction of the βγ subunit with channels, as observed in other signalling systems tested so far (Rhim and Miller 1994, Wilding et al. 1995, Kim et al. 1997, Soldo and Moises 1997, Connor et al. 1999, Chieng and Bekkers 2001, Lee et al. 2004). This type of signal transduction is sometimes described as "membrane delimited" to emphasize the fact that it is mediated by the βγ subunit in the plane of the plasma membrane (for reviews, see Kim et al. 1997, Kaneko et al. 1999). Membrane-delimited inhibition of Ca^{2+} channels is relieved by a large membrane depolarisation, which disrupts the connections of the βγ subunits and the channels (Ikeda 1996, Meir et al. 2000).

To test this possibility, we evoked Ca^{2+} currents before and after a large depolarising pulse. It was found that DAMGO-induced inhibition was still present after a large membrane depolarisation, suggesting that Ca^{2+} channels were not inhibited by the βγ subunit in a conventional membrane-delimited mode.

However, Ca^{2+} channels undergo time-dependent inactivation, i.e., Ca^{2+} current amplitude decreases when a sustained depolarising voltage is applied (as seen in all figures in this manuscript). It has been suggested that this type of inactivation is caused by Ca^{2+} ions themselves that enter the cell during a voltage step (Brehm and Eckert 1978). The process of time-dependent inactivation of Ca^{2+} channels could mask the "de-inhibition" of Ca^{2+} channels caused by the large amplitude depolarisation. In order to avoid Ca^{2+} dependent channel inhibition, we replaced Ca^{2+} ions with Ba^{2+} ions as a charge carrier. Inward Ba^{2+} currents flowing into the cell through the Ca^{2+} channels show much less time-dependent inactivation than Ca^{2+} currents (Goo et al. 2006).

Indeed, we demonstrated that without DAMGO application, Ba^{2+} currents increased after a large voltage step in the majority of cases. This may suggest that Ca^{2+} channels are continuously inhibited by βγ released tonically from G proteins. The existence of such tonic inhibition of Ca^{2+} channels has been demonstrated by others (for reviews, see Kim et al. 1997, Kaneko et al. 1999). During DAMGO application, the amplitude of the Ba^{2+} current also increased after the voltage step compared to the control. The amplitude increase was similar to that seen after a large voltage step without

DAMGO application. Because the magnitude of the Ba^{2+} current increase after the large voltage step was the same in the presence or absence of DAMGO, we concluded that the process was DAMGO-independent. Once the Ba^{2+} current increased following a large voltage step, its amplitude promptly began to show time-dependent inactivation in the presence as well as in the absence of DAMGO. We presume that immediately after the voltage step, the connections between the βγ subunits and the channels were disrupted and channel inhibition was relieved. This was followed by recovery of the inhibition due to reconnection of βγ subunits with the channels. Indeed, others have found that the ability of large membrane depolarisations to relieve inhibition is short-lived (Golard and Siegelbaum 1993, Toselli et al. 1999).

The important finding was that DAMGO-induced inhibition of Ca^{2+} channels (measured as Ba^{2+} current) was still present after a large voltage step, suggesting that Ca^{2+} channels were not inhibited exclusively in a "membrane-delimited mode". We suspected that cytoplasmic second messengers might be involved in DAMGO-induced inhibition of Ca^{2+} channels.

To confirm the involvement of cytoplasmic second messengers, we performed experiments in the cell-attached configuration. The pipette was loaded with Ba^{2+} ions as the charge carrier through Ca^{2+} channels in the patched membrane and DAMGO was applied to the cell from the outside of the pipette. The macroscopic Ba^{2+} current was evoked by ramp depolarisation of the patched membrane similarly to other studies (Bargas et al. 1994). In such an experimental configuration, the distance between the μ opioid receptors and Ca^{2+} channels is too great to account for Ca^{2+} channel inhibition by a membrane-delimited process (Lei et al. 2001). We found that macroscopic Ba^{2+} patch currents through the Ca^{2+} channels were very effectively inhibited by DAMGO. This constitutes strong evidence that Ca^{2+} channels are inhibited through a transduction process involving cytoplasmic second messengers.

Is PKA and/or PKC involved in modulation of Ca^{2+} currents?

The α subunit of voltage-gated Ca^{2+} channels possesses PKA and PKC phosphorylation sites (Ahlijanian et al. 1991, Hell et al. 1995, Wu et al. 2006). Therefore, the possibility that PKA and/or PKC participate in the transduction pathway from μ opioid receptors to Ca^{2+} channels was considered.

Classical evidence indicates that tonic channel phosphorylation is required to prevent down-regulation of Ca^{2+} currents (Doroshenko et al. 1982, Forscher et al. 1986). These studies, implicated cAMP and PKA in tonic Ca^{2+} channel phosphorylation. It seems that the same mechanism supports Ca^{2+} channel activity in mPFC pyramidal neurons. In our study, inhibition of adenylyl cyclase and/or PKA itself markedly decreased Ca^{2+} current activity. Moreover, activation of PKA in mPFC pyramidal neurons by the adenylyl cyclase stimulator forskolin (Chijiwa et al. 1990) did not enhance Ca^{2+} currents, which suggests that the positive modulatory effect of the cAMP/PKA pathway on Ca^{2+} channels is saturating under basal conditions in mPFC pyramidal neurons.

We applied the drug H-89 in order to inhibit PKA directly (Vargas and Lucero 2002). Application of DAMGO alone or together with different concentrations of H-89 decreased Ca^{2+} current amplitude to exactly the same level, suggesting that inhibition by DAMGO and inhibition of PKA were not additive processes. When PKA was progressively inhibited with higher doses of H-89, Ca^{2+} current amplitude decreased, in agreement with the assumption that Ca^{2+} channel activity depends on its tonic phosphorylation by PKA. As higher concentrations of H-89 led to greater decreases in current amplitude, the amount by which DAMGO inhibited Ca^{2+} current also decreased progressively. Finally, when high doses of the PKA inhibitor were applied, DAMGO did not inhibit Ca^{2+} current. This suggests that DAMGO-induced inhibition depends on the availability of active PKA: the less PKA available due to inhibition by H-89, the smaller the inhibitory effect of DAMGO.

Classical evidence suggests that activation of μ opioid receptors inhibits adenylyl cyclase, a natural PKA activator (Chieng and Williams 1998, Ingram et al. 1998). Therefore, one may presume that the cAMP/PKA pathway is involved in inhibition of Ca^{2+} currents in mPFC pyramidal neurons. The complete pathway in mPFC pyramidal neurons would involve activation of μ opioid receptors, which inhibit adenylyl cyclase, leading to deactivation of PKA and dephosphorylation of N-type Ca^{2+} channels by phosphatases.

The adenylyl cyclase/PKA transduction system operates in many eukaryotic cells (Tasken and Aandahl 2003). A similar intracellular transduction system has

recently been described in cardiac sympathetic nerve endings, where activation of H3 receptors leads to inhibition of adenylyl cyclase, decreased PKA activity and suppression of N-type Ca^{2+} currents (Seyedi et al. 2005).

Recent results from our laboratory indicate that DAMGO has no appreciable effect on voltage-dependent Na^{+} currents in mPFC pyramidal neurons (Witkowski and Szulczyk 2006). It is likely that the element of the transduction pathway in pyramidal neurons that conveys signals to Ca^{2+} channels – whether a G-protein, adenylyl cyclase (Hanoune and Defer 2001), PKA (Skalhegg and Tasken 1997) or another molecule – does not signal to Na^{+} channels.

We found that activation of PKC by PMA (Chen and Yu 1994) or inhibition of PKC by chelerythrine chloride (Herbert et al. 1990) failed to affect DAMGO-induced inhibition of Ca^{2+} current. Therefore, PKC is probably not involved in the transduction pathway from μ opioid receptors to Ca^{2+} channels.

CONCLUSION

We conclude that activation of μ opioid receptors in medial prefrontal cortex pyramidal neurons inhibits N type Ca^{2+} channel currents, and that protein kinase A is involved in this transduction pathway.

ACKNOWLEDGEMENTS

Supported by grant no. KBN-033/P05/2000, no. KBN-0575/P05/2005/28, FW5/N/2007. We thank Mrs. Izabella Zaborowska and Mrs. Marta Kuźniarska for technical assistance.

REFERENCES

Ahlijanian MK, Striessnig J, Catterall WA (1991) Phosphorylation of an alpha 1-like subunit of an omega-conotoxin-sensitive brain calcium channel by cAMP-dependent protein kinase and protein kinase C. J Biol Chem 266: 20192–20197.

Bargas J, Howe A, Eberwine J, Cao Y, Surmeir DJ (1994) Cellular and molecular characterization of Ca^{2+} currents in acutely isolated, adult rat neostriatal neurons, J Neurosci 14: 6667–6686.

Berger B, Gaspar P, Verney C (1991) Dopaminergic innervation of the cerebral cortex: unexpected differences between rodents and primates. Trends Neurosci 14: 21–27.

Brehm P, Eckert R (1978) Calcium entry leads to inactivation of calcium channel in Paramecium. Science 202: 1203–1206.

Carafoli E (2002) Calcium signalling: A tail for all seasons. Proc Natl Acad Sci U S A 99: 1115–1122.

Carr DB, O'Donell P, Card JP, Sesack SR (1999) Dopamine terminals in the rat prefrontal cortex synapse on pyramidal cells that project to the nucleus accumbens. J Neurosci 19: 11049–11060.

Carr DB, Sesack SR (2000) Projections from he rat prefrontal cortex to the ventral tegmental area: target specificity in the synaptic associations with mesoaccumbens and mesocortical neurons. J Neurosci 20: 3864–3873.

Chen Y, Yu L (1994) Differential regulation by cAMP-dependent protein kinase and protein kinase C of the μ-opioid receptor coupling to a G protein-activated K^{+} channel. J Biol Chem 269: 7839–7842.

Chieng B, Williams JT (1998) Increased opioid inhibition of GABA release in nucleus accumbens during morphine withdrawal. J Neurosci 18: 7033–7039.

Chieng B, Bekkers JM (2001) Inhibition of calcium channels by opioid- and adenosine-receptor agonists in neurons of the nucleus accumbens. Br J Pharmacol 133: 337–344.

Chijiwa T, Mishima A, Hagiwara M, Sano M, Hayashi K, Inoue T, Naito K, Toshioka T, Hidaka H (1990) Inhibition of forskolin-induced neurite outgrowth and protein phosphorylation by a newly synthesized selective inhibitor of cyclic AMP-dependent protein kinase, N-[2-(p-bromocinnamylamino)ethyl]-5-isoquinoline sulfonamide (H-89), of PC12D pheochromocytoma cells. J Biol Chem 265: 5267–5272.

Connor M, Schuller A, Pintar JE, Christi MJ (1999) Mu opioid receptor modulation of calcium channel current in periaqueductal grey neurons from C57B16/J mice and mutant mice lacking MOR1. Br J Pharmacol 126: 1553–1558.

Day M, Olson PA, Platzer J, Striessnig J, Surmeier DJ (2002) Stimulation of 5-HT2 receptors in prefrontal pyramidal neurons inhibits $Ca_v1.2$ L-type Ca^{2+} currents via a PLCβ/IP3/calcineurin signaling cascade. J Neurophysiol 87: 2490–2504.

Doroshenko PA, Kostyuk PG, Martynyuk AE (1982) Intracellular metabolism of adenosine 3',5'-cyclic monophosphate and calcium inward current in perfused neurones of Helix pomatia. Neuroscience 7: 2125–2134.

Forscher P, Oxford GS, Schulz D (1986) Noradrenaline modulates calcium channels in avian dorsal root ganglion cells through tight receptor-channel coupling. J Physiol 379: 131–144.

Golard A, Siegelbaum SE, (1993) Kinetic basis for the voltage-dependent inhibition of N-type calcium current by somatostatin and norepinephrine in chick sympathetic neurons. J Neurosci 13: 3884–3894.

Goo YS, Lim W, Elmslie KS, (2006) Enhances U-type inactivation of N-type (Cav2.2) calcium current in rat sympathetic neurons. J Neurophysiol 96: 1075–1083,

Hanoune J, Defer N (2001). Regulation and role of adenylyl cyclase isoforms. Annu Rev Pharmacol Toxicol 41: 145–174.

Hell JW, Yokoyama CT, Breeze LJ, Chavkin C, Catterall WA (1995) Phosphorylation of presynaptic and postsynaptic calcium channels by cAMP-dependent protein kinase in hippocampal neurons.EMBO J 14: 3036–3044.

Herbert JM, Augereau JM, Gleye J, Maffrand JP (1990) Chelerythrine is a potent and specific inhibitor of protein kinase C. Biochem Biophys Res Commun 172: 993–9.

Holz GG4th, Rane SG, Dunlap K (1986) GTP-binding proteins mediate transmitter inhibition of voltage-dependent calcium channels. Nature 319: 670–672.

Ikeda SR (1996) Voltage-dependent modulation of N-type calcium channels by G protein bgamma subunits. Nature 380: 255–258.

Ingram SL, Vaughan CW, Bagley EE, Connor M, MacDonald JC (1998) Enhanced opioid efficacy in opioid dependence is caused by an altered signal transduction pathway. J Neurosci 18: 10269–10276.

Ishibashi H, Rhee JS, Akaike N (1997) Effect of nilvadipine on high-voltage activated Ca^{2+} channels in rat CNS neurons. Neuroreport 8: 853–857.

Kaneko S, Akaike A, Satoh μ (1999) Receptor-mediated modulation of voltage-dependent Ca^{2+} channels via heterotrimeric G-proteins in neurons. Jpn J Pharmacol 81: 324–331.

Kim CJ, Rhee JS, Akaike N (1997) Modulation of high-voltage activated Ca^{2+} channels in the rat periaqueductal gray neurons by μ-type opioid agonist. J Neurophysiol 77: 1418–1424.

Kolb B (1984) Functions of the frontal cortex of the rat: a comparative review. Brain Res 320: 65–98.

Kukwa W, Macioch T, Szulczyk PJ (1998) Stellate neurons innervating the heart express N, L and P/Q calcium channels in rats. J Autonom Nerv Syst 74: 143–151.

Kukwa W, Macioch T, Rola R, Szulczyk P (2000) Kinetic and pharmacological properties of Ca^{2+} currents in postganglionic sympathetic neurones projecting to muscular and cutaneous effectors. Brain Res 873: 173–180.

Lee JJ, Hahm ET, Min BI, Cho YW (2004) Activation of protein kinase C antagonizes the opioid inhibition of calcium current in rat spinal dorsal horn neurons. Brain Res 1017: 108–119.

Lei Q, Talley EM, Bayliss DA (2001) Receptor-mediated inhibition of G protein-coupled inwardly rectifying potassium channels involves Gaq family subunits, phospholipase C, and a readily diffusible messenger. J Biol Chem 276: 16720–16730.

Lorenzon NM, Foehring RC (1995) Characterization of pharmacologically identified voltage-gated calcium channel currents in acutely isolated rat neocortical neurons. II. Postnatal development. J Neurophysiol 73: 1443–1451.

Manoach DS (2003) Prefrontal cortex dysfunction during working memory performance in schizophrenia: reconciling discrepant findings. Schizophr Res 60: 285–298.

Mansour A, Fox CA., Akil H, Watson SJ (1995) Opioid-receptor mRNA expression in the rat CNS: anatomical and functional implications. Trends Neurosci 18: 22–29.

Meir A, Bell DC, Stephens GJ, Page KM, Dolphin AC (2000) Calcium channel b subunit promotes voltage-dependent modulation of α1B by G$\beta\gamma$. Biophys J 79: 731–746.

Öngür D, Price JL (2000) The organization of networks within the orbital and medial prefrontal cortex of rats, monkeys and humans. Cereb Cortex 10: 206–219.

Rhim H, Miller RJ (1994) Opioid receptors modulate diverse types of calcium channels in the nucleus tractus solitarius of the rat. J Neurosci 14: 7608–7615.

Ribeiro SC, Kennedy SE, Smith YR, Stohler CS, Zubieta JK (2005) Interface of physical and emotional stress regulation through the endogenous opioid system and mu-opioid receptors. Prog Neuropsychopharmacol Biol Psychiatry 29: 1264–1280.

Rola R, Szulczyk PJ, Witkowski G (2003) Voltage-dependent Ca^{2+} currents in rat cardiac dorsal root ganglion neurons. Brain Res 961: 171–178.

Rosen HJ, Allison SC, Schauer GF, Gorno-Tempini ML, Weiner MW, Miller BL (2005) Neuroanatomical correlates of behavioural disorders in dementia. Brain 128: 2612–2625.

Rusin KI, Moises HC (1995) Mu opioid receptor activation reduces multiple components of high-threshold calcium current in rat sensory neurons. J Neurosci 15: 4315–4327.

Schmidt P, Schmolke C, Musshoff F, Prohaska C, Menzen M, Madea B (2001) Numerical density of mu-opioid receptor expressing neurons in the frontal cortex of drug related fatalities. Forensic Sci Int 115: 219–229.

Schmidt P, Schmolke C, Musshoff F, Menzen M, Prohaska C, Madea B (2003) Area-specific increased density of mu-opioid receptor immunoreactive neurons in the cerebral cortex of drug-related fatalities. Forensic Sci Int 133: 204–211.

Seyedi N, Mackins CJ, Machida T, Reid AC, Silver RB, Levi R (2005) Histamine H3 receptor induced attenuation of norepinephrine exocytosis: a decrease protein kinase A activity mediates a reduction in intracellular calcium, J Pharm Exp Ther 312: 272.

Skalhegg BS, Tasken K (1997) Specificity in the cAMP/PKA signaling pathway. Differential expression, regulation, and subcellular localization of subunits of PKA. Front Biosci 2:331–342.

Soldo BL, Moises HC (1997) Mu-opioid receptor activation decreases N-type Ca^{2+} current in magnocellular neurons of the basal forebrain. Brain Res 758: 118–126.

Stewart AE, Yan Z, Surmeier DJ, Foehring RC (1999) Muscarine modulates Ca^{2+} channel currents in rat sensorimotor pyramidal cells via two distinc pathways. J Neurophysiol 81: 72–84.

Tasken K, Aandahl EM (2003) Localized effects od cAMP mediated by distinct routes of protein kinase A. Physiol Rev 84: 137–167.

Toselli M, Tosseti P, Taglietti V (1999) Kinetic study of N-type calcium current modulation by μ-opioid receptor activation in the mammalian cell lLine NG108-15. Biophys J 76: 2560–2574

Vargas G, Lucero MT (2002) Modulation by PKA of the hyperpolarization-activated current (Ih) in cultured rat olfactory receptor neurons. J Membr Biol 188: 115–125.

Verheugen JAH, Fricker D, Miles R (1999) Noninvasive measurements of the membrane potential and GABAergic action in hippocampal interneurons. J Neurosci 19: 2546–2555.

Wilding TJ, Womack MD, McCleskey EW (1995) Fast, local signal transduction between the mu opioid receptor and Ca^{2+} channels. J Neurosci 15: 4124–4132.

Williams GV, Castner SA (2006) Under the curve: critical issues for elucidating D1 receptor function in working memory. Neurosci 139: 263–276.

Witkowski G, Szulczyk P (2006) Opioid μ receptor activation inhibits sodium currents in prefrontal cortical neurons via a protein kinase A- and C-dependent mechanism. Brain Res 1094: 92–106.

Wu ZQ, Li M, Chen J, Chi ZQ, Liu JG (2006) Involvement of cAMP/cAMP-dependent protein kinase signaling pathway in regulation of Na^{+},K^{+}-ATPase upon activation of opioid receptors by morphine. Mol Pharmacol 69: 866–876.

Zubieta JK, Smith YR, Bueller JA, Xu Y, Kilbourn MR, Jewett DM, Meyer CR, Koeppe RA, Stohler CS (2002) μ-Opioid receptor-mediated antinociceptive responses differ in men and women. J Neurosci 22: 5100–5107.

Zubieta JK, Ketter TA, Bueller JA, Xu Y, Kilbourn MR, Young EA, Koeppe RA (2003) Regulation of human affective responses by anterior cingulate and limbic m-opioid neurotransmission. Arch Gen Psychiatry 60: 1145–1153.